

## Pomeron loops in zero transverse dimensions

Arif I. Shoshi<sup>1,2,\*</sup> and Bo-Wen Xiao<sup>1,†</sup><sup>1</sup>*Department of Physics, Columbia University, New York, NY, 10027, USA*<sup>2</sup>*Fakultät für Physik, Universität Bielefeld, D-33501 Bielefeld, Germany*

(Dated: December 16, 2017)

We analyze a toy model which has a structure similar to that of the recently found QCD evolution equations, but without transverse dimensions. We develop two different but equivalent methods in order to compute the leading-order and next-to-leading order Pomeron loop diagrams. In addition to the leading-order result which has been derived within other toy models [1, 2], we can also calculate the next-to-leading order contribution which provides the ( $\alpha_s^2 \alpha Y$ ) correction. We interpret this result and discuss its possible implications for the four-dimensional QCD evolution.

PACS numbers: 12.38.Cy; 11.10.Hi; 11.55.Bq

## I. INTRODUCTION

There have been major breakthroughs in understanding high-density QCD evolution recently. Several important observations have been made: (i) gluon number fluctuations have a big effect on the evolution towards gluon saturation [3], (ii) a connection between high-energy QCD evolution and statistical physics models of reaction-diffusion type was found [4, 5] which has clarified the interpretation of fluctuations in an event-by-event picture, and (iii) it was realized that the relevant fluctuations are missed [6] by the existing Balitsky-JIMWLK equations [7, 8]. These observations have led to the creation of new QCD evolution equations which include gluon number fluctuations or Pomeron loops [9, 10, 11, 12].

The new equations describe the usual BFKL evolution, Pomeron splittings and Pomeron mergings and, thus, through iterations, Pomeron loops. A lot is known about the structure of the new equations [13, 14, 15, 16, 17], however, because of their complexity, little about their solutions. So far, analytical results for the energy dependence of the saturation momentum and for the scaling behavior of the  $T$ -matrix at asymptotic energies [3, 6] and some numerical simulations of approximations to the exact equations [17, 18] are available. Solutions to the new equations in the range of collider energies are desired.

In this paper, we consider a toy model which has a structure similar to that of the new QCD evolution equations, but which has no transverse dimensions. This simplification allows an exact solution of the evolution equations. The particle-particle scattering amplitude is calculated. The effects of saturation and unitarity, or “Pomeron” loops which are the characteristics of the new evolution equations, are investigated.

A decade ago, Mueller [1] studied a similar toy model without transverse dimensions which was motivated by the QCD dipole model [19]. He has been able to solve the toy model exactly and calculate the  $S$ -matrix. Ob-

servations made by studying this toy model (e.g. the one that fluctuations in particle numbers lead to a divergent multiple scattering series) have been shown numerically [20, 21] to be valid also in the four-dimensional QCD. The hope that some of the results obtained in the toy model discussed in this paper may also apply in four-dimensional QCD is one of the motivations for this work.

In the toy model proposed by Mueller [1], particle-particle scattering in the center-of-mass frame at total rapidity  $Y$  was considered. In this model, each particle evolves to a dense system through particle branching (splitting). Unitarity effects (at leading order accuracy) are correctly described due to the multiple scatterings between the dense systems. There are no particle mergings in the wavefunctions of the particles in this model, therefore, the model fails to describe saturation effects in the wavefunctions of the particles which become important at very high rapidities  $Y > Y_s = \frac{2}{\alpha_s^2} \ln \frac{1}{\alpha_s^2}$ . In the language of loops, only the loops stretching over the rapidity interval greater than  $Y/2$  (“large” loops) shown e.g. in Fig. 1B are included (at leading-order accuracy and for  $Y < Y_s$ ). “Large” loops are created by matching the evolution (“Pomeron” splittings) of both particle’s wavefunctions at  $Y/2$ . However, there are no loops inside the particle’s wavefunctions (“small” loops) where the “Pomeron” splits and merges, as shown e.g. in Fig. 1C (see, e.g. ref.[22]), within the rapidity interval  $Y/2$ . The above limitations of the toy model are, of course, properties of the QCD dipole model [19] as well and are well-known.

Mueller’s toy model breaks down at  $Y \simeq Y_s$ . In a later work Mueller and Salam [2] did include saturation effects by imposing boost invariance on the small- $x$  evolution in a toy model, getting an expression for the  $S$ -matrix which is valid also for  $Y > Y_s$ . The effect of saturation was an extension of the validity region of the result obtained for  $Y < Y_s$  in [1] also to the region where  $Y > Y_s$ .

Our toy model which is inspired by the new QCD evolution equations [9, 10, 11, 12] allows us to study unitarity effects as well as saturation effects in a more refined and systematic way. We calculate the leading order (LO) and the next-to-leading order (NLO) loop contributions

\*Electronic address: shoshi@physik.uni-bielefeld.de

†Electronic address: bowen@phys.columbia.edu

to the particle-particle scattering amplitude. The LO result, which is the LO contribution of the “large” loops, agrees with the results from [1, 2]. Our NLO result consisting of the NLO contribution of the “large” loops and the LO contribution of the “small” loops is new. The NLO correction with respect to the LO result is of order  $\alpha_s^2 \alpha Y$ . This is the main result of the paper. It tells us that the NLO contribution is negligible as compared with the LO contribution up to rapidities  $Y \leq 1/\alpha \alpha_s^2$ .

Our LO result agrees with the result derived within Mueller’s toy model up to  $Y \simeq Y_s$ . Beyond  $Y_s$  Mueller’s toy model fails to include saturation effects. The result in [2] which involves saturation effects is the same as our LO result until  $Y \simeq 1/\alpha \alpha_s^2$  which is parametrically much larger than  $Y_s$ . However, beyond  $Y \simeq 1/\alpha \alpha_s^2$  the NLO corrections become important which are not taken into account in Mueller and Salam’s toy model [2].

Presumably our toy model reveals the properties of the four-dimensional QCD evolution to some extent. In fact, its behavior is a heuristic sign that the NLO contribution can be neglected in the QCD evolution as well as long as  $Y \ll 1/\alpha \alpha_s^2$ . Such a NLO correction seems to appear also in real QCD. Considering the one-loop diagram for example, the LO contribution in QCD is  $(\alpha_s^2)^2 \exp(2\alpha Y)$  which comes from varying the size of the loop from 0 to  $Y$ , where  $\alpha = \alpha_P - 1 = \frac{4\alpha_s N_c}{\pi} \ln 2$ . The NLO contribution  $(\alpha_s^2)^2 \alpha Y \exp(\alpha Y)$  comes from changing the location of a fixed zero-size loop from 0 to  $Y$ . The suppression of the NLO contribution by the factor  $\alpha Y/e^{\alpha Y}$  directly leads to the general correction  $\alpha_s^2 \alpha Y$  (the same happens in our toy model).

The paper is organized as follows: In Sec. II, we show the toy model. Two methods are developed in order to solve the toy model and some discussion is provided on the consequences of the NLO corrections. They are explained in Sec. III. In the Appendices we show the Lorentz-invariance of the toy model and give the solution to another commonly used zero-dimensional model. Finally, we discuss the results and give the conclusions.

## II. A TOY MODEL WITH “POMERON” LOOPS

In this section, we consider a toy model without transverse dimensions which has a structure similar to that of the recently found four-dimensional QCD evolution equation [9, 10, 11, 12]. The toy model describes the rapidity evolution of the particle number  $n$  of a system. The dynamics in zero-transverse dimensions is given by the following Langevin equation<sup>1</sup>

$$\frac{d\tilde{n}}{dy} = \alpha \tilde{n} - \beta \tilde{n}^2 + \sqrt{2\alpha \tilde{n}} \nu(y) \quad (1)$$

<sup>1</sup> We provide the solution to the zero transverse dimensional sFKPP equation with a different noise term  $\sqrt{2(\alpha \tilde{n} - \beta \tilde{n}^2)} \nu(y)$  in Appendix. B

where  $\nu(y)$  is a Gaussian white noise:  $\langle \nu(y) \rangle = 0$  and  $\langle \nu(y) \nu(y') \rangle = \delta(y - y')$ . Eq. (1) is known as the zero transverse dimensional “Reggeon field theory” equation and it contains the projectile-target duality (see Appendix A). The structure of Eq. (1) is obvious: the first term on the r.h.s. represents the growing of the particles, the second term describes particle recombinations which limit the growth at a maximum occupancy, and the third term describes the particle number fluctuations. These are essentially the main ingredients of the real QCD equations.

With Ito’s calculus, one can write Eq. (1) into an infinite hierarchy of coupled evolution equations,

$$\frac{dn^{(k)}}{dy} = k \alpha n^{(k)} + k(k-1) \alpha n^{(k-1)} - k \beta n^{(k+1)}, \quad (2)$$

where  $n^{(k)} = \langle : \tilde{n}^k : \rangle$  is the expectation value of  $k$ -particles during the evolution and it should be understood as a normal ordered number operator (i.e. the factorial moment  $\langle \tilde{n}(\tilde{n}-1) \cdots (\tilde{n}-k+1) \rangle$ ) according to its physical interpretation. Here,  $k \alpha n^{(k)}$  is the growth term,  $k(k-1) \alpha n^{(k-1)}$  the fluctuation term, and  $k \beta n^{(k+1)}$  the recombination term. Eqs. (1, 2) are the zero-transverse-dimensional analog of the real QCD equations (see [6, 10]). A simple derivation and a discussion in the context of QCD evolution of eqs. (1, 2) can be found in [6]. The solution to another widely discussed Langevin equation is shown in Appendix B.

## III. SOLUTION TO THE TOY MODEL

Eq. (2) is quite complicated since  $n^{(k)}$  is coupled with  $n^{(k-1)}$  and  $n^{(k+1)}$  in the evolution, i.e., Eq. (2) is just a particular equation within an infinity hierarchy of coupled equations. However, the following observation helps to solve Eq. (2): one can neglect the recombination term if one starts with a dilute object at the beginning of rapidity evolution, on the other hand, one can see that  $n^{(k)} = (\alpha/\beta)^{(k)}$  is an approximate fixed point of Eq. (2) in extremely high rapidity and  $\frac{\beta}{\alpha} = \alpha_s^2 \ll 1$  limit. This will be more clear if one thinks about this in terms of the evolution equation of  $T^{(k)}$  (one can define  $T^{(k)} = (\alpha_s^2)^k n^{(k)}$ ):  $\frac{dT^{(k)}}{dy} = \alpha [kT^{(k)} - kT^{(k+1)} + k(k-1)\alpha_s^2 T^{(k-1)}]$ , in which it is easy to find  $\lim_{Y \rightarrow \infty} T^{(k)} = 1$ . Therefore, if one starts with a dilute object at  $Y = 0$  ( $n \ll n_s = 1/\alpha_s^2$ ), then one can consider the evolution equation without the recombination term at the early stages of the evolution, and turn on the recombination term as a perturbation at the end of the evolution which forms the “Pomeron” loops. Following this philosophy, we have found two different methods to solve Eq. (2) which we will present in the following subsections. Before entering the calculations, we should state that we always work in a parametrical limit in which  $\alpha_s^2 \rightarrow 0$  and  $\alpha Y \rightarrow \infty$ , but  $\alpha_s^2 e^{\alpha Y}$  is fixed and finite.

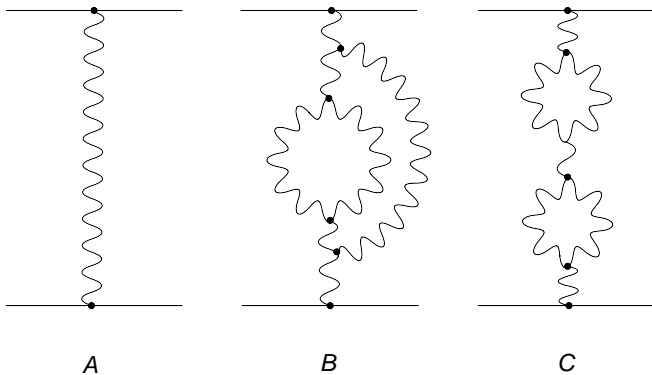


FIG. 1: Three kinds of reggeon graphs, in which the curly lines represent BFKL ladders. Diagram (A) is a simple BFKL ladder exchanged between the two particles (horizontal lines); Diagram (B) is the LO Pomeron loop diagram which has been calculated in ref. [1, 2, 21]; Diagram (C) is the NLO pomeron loop diagram which was not included in the dipolar approach of ref. [1, 2, 21] while it can be computed in this toy model.

### A. Method I: Integral Representation

Eq. (2) without the recombination term,

$$\frac{dn_0^{(k)}}{dy} = k\alpha n_0^{(k)} + k(k-1)\alpha n_0^{(k-1)}, \quad (3)$$

can be solved exactly if given some physically chosen initial conditions. In this paper, we consider the evolution of a single particle for which the initial conditions are  $n_0^{(1)}|_{y=0} = N$  and  $n_0^{(k)}|_{y=0}^{k>1} = 0$ . The solution to Eq. (3) with the above initial conditions reads

$$n_0^{(k)}(y) = N k! e^{k\alpha y} (1 - e^{-\alpha y})^{k-1} \quad (4)$$

and corresponds to the  $k$ -particle density obtained via splitting from a single particle after the evolution over the rapidity  $y$ . To turn on the perturbation, let us start with the first equation in the infinite hierarchy (2),

$$\frac{dn_1^{(1)}}{dy} = \alpha n_1^{(1)} - \beta n_0^{(2)}, \quad (5)$$

which has the solution

$$\begin{aligned} n_1^{(1)}(Y) &= n_0^{(1)}(Y) - \beta \int_0^Y dy e^{\alpha(Y-y)} n_0^{(2)}(y) \\ &= N e^{\alpha Y} - 2 \frac{\beta}{\alpha} N e^{2\alpha Y} \left(1 - \frac{\alpha Y}{e^{\alpha Y}} - \frac{1}{e^{\alpha Y}}\right). \end{aligned} \quad (6)$$

It is straight forward to recognize that the first term in Eq. (6) is the usual BFKL term, and the second term corresponds to the one-loop diagram with the right intrinsic minus sign. One can also see that  $\frac{\alpha Y}{e^{\alpha Y}}$  is the NLO contribution in the parametrical limit we mentioned above.

To get the LO two-loop diagram shown in Fig. 1 B, we start with the second equation in Eq. (2),

$$\frac{dn_1^{(2)}}{dy} = 2\alpha n_1^{(2)} + 2\alpha n_0^{(1)} - 2\beta n_0^{(3)}, \quad (7)$$

whose solution is

$$\begin{aligned} n_1^{(2)}(Y) &= n_0^{(2)}(Y) - 2\beta \int_0^Y dy e^{2\alpha(Y-y)} n_0^{(3)}(y) \\ &= 2N e^{2\alpha Y} (1 - e^{-\alpha Y}) - 2 \cdot 3! \frac{\beta}{\alpha} N e^{3\alpha Y} \left(1 - \frac{2\alpha Y}{e^{\alpha Y}} + \dots\right), \end{aligned} \quad (8)$$

then turn on the perturbation,  $\frac{dn_2^{(1)}}{dy} = \alpha n_2^{(1)} - \beta n_1^{(2)}$ , in order to take into account the recombination from  $n^{(2)}$  to  $n^{(1)}$  (in addition to the recombination from  $n_0^{(3)}$  to  $n^{(2)}$  given by Eq. (7)), which leads to

$$\begin{aligned} n_2^{(1)}(Y) &= n_0^{(1)}(Y) - \beta \int_0^Y dy e^{\alpha(Y-y)} n_1^{(2)}(y) \\ &= N e^{\alpha Y} - 2 \frac{\beta}{\alpha} N e^{2\alpha Y} \left(1 - \frac{\alpha Y}{e^{\alpha Y}} - \frac{1}{e^{\alpha Y}}\right) + 3! \left(\frac{\beta}{\alpha}\right)^2 N e^{3\alpha Y} \left(1 - \frac{4\alpha Y}{e^{\alpha Y}} + \mathcal{O}\left(\frac{1}{e^{\alpha Y}}\right)\right). \end{aligned} \quad (9)$$

The third term in Eq. (9) represents the LO two-loop diagram shown in Fig. 1 B.

In order to calculate the NLO two-loop diagram shown in Fig. 1 C, one has to enforce a recombination to happen after a splitting. Thus, starting with  $n_0^{(1)} = N e^{\alpha Y}$ , one splitting given by  $n_2^{(0)}(Y) = 2\alpha \int_0^Y dy e^{2\alpha(Y-y)} n_0^{(1)}(y)$ , followed by one merging  $\Delta n_1^{(1)} = -\beta \int_0^Y dy e^{\alpha(Y-y)} n_0^{(2)}(y)$ , yields the result for the one-loop diagram. A further splitting and a subsequent merging gives the result for the NLO two-loop diagram,

$$\Delta n^{(1)}(Y) = 3! \left(\frac{\beta}{\alpha}\right)^2 N e^{3\alpha Y} \left(\frac{2}{3} \frac{\alpha Y}{e^{\alpha Y}} + \mathcal{O}\left(\frac{1}{e^{\alpha Y}}\right)\right). \quad (10)$$

In fact, in order to calculate any loop diagram, one just needs to know the merging and splitting vertices which according to Eq. (2) read, respectively,

$$\Delta n_m^{(k)}(Y) = -k\beta \int_0^Y dy e^{k\alpha(Y-y)} \Delta n^{(k+1)}(y), \quad (11)$$

$$\Delta n_s^{(k)}(Y) = k(k-1)\alpha \int_0^Y dy e^{k\alpha(Y-y)} \Delta n^{(k-1)}(y). \quad (12)$$

For particle-particle scattering, the  $(k+1)$ -th order diagram contains  $k$ -splittings and  $k$ -mergings: The leading-order diagram corresponds to the diagram in which all  $k$ -splittings occur before all the  $k$ -mergings, the next-to-leading order diagram is always the diagram in which exactly one merging takes place before one splitting. The sum over all LO and NLO loop diagrams gives the LO and NLO contributions to the  $T$ -matrix, respectively.

For particle-particle scattering, the sum over the LO loop diagrams (leading and next-to-leading contribution) reads

$$n_{LO}^{(1)}(Y) = \sum_{k=1}^{\infty} (-1)^{k+1} N \cdot k! e^{k\alpha Y} \left(\frac{\beta}{\alpha}\right)^{k-1} \left(1 - (k-1)^2 \frac{\alpha Y}{e^{\alpha Y}} + \mathcal{O}\left(\frac{1}{e^{\alpha Y}}\right) + \mathcal{O}\left(\left(\frac{\alpha Y}{e^{\alpha Y}}\right)^2\right)\right), \quad (13)$$

while the sum over the NLO loop diagrams (leading contribution) is

$$n_{NLO}^{(1)}(Y) = \sum_{k=1}^{\infty} (-1)^{k+1} N \cdot k! e^{k\alpha Y} \left(\frac{\beta}{\alpha}\right)^{k-1} \left(\frac{(k-1)(k-2)^2}{k} \frac{\alpha Y}{e^{\alpha Y}} + \mathcal{O}\left(\frac{1}{e^{\alpha Y}}\right) + \mathcal{O}\left(\left(\frac{\alpha Y}{e^{\alpha Y}}\right)^2\right)\right). \quad (14)$$

The resulting  $S$ -matrix,  $S \equiv 1 - T$  (with  $T = \alpha_s^2(n_{LO}^{(1)} + n_{NLO}^{(1)})$ ), which includes LO and NLO loop diagrams, can be written in the form

$$S(Y) = \sum_{k=0}^{\infty} (-1)^k \cdot k! (\alpha_s^2 e^{\alpha Y})^k \left\{1 + \alpha_s^2 \alpha Y \cdot (3k^2 - k) + \alpha_s^2 \cdot f_1(k) + (\alpha_s^2 \alpha Y)^2 \cdot f_2(k) + \dots\right\}, \quad (15)$$

where we have put  $\frac{\beta}{\alpha} = \alpha_s^2$  in close analogy with the four-dimensional QCD and  $N = 1$ .  $f_1(k)$  and  $f_2(k)$  are functions of  $k$ , which are too complicated to be calculated in this method. The series in Eq. (15) is a divergent series, however, it is Borel-summable. After the Borel-summation, the expression for the  $S$ -matrix becomes rather complicated,

$$\begin{aligned} S(Y) &= \frac{1}{\alpha_s^2 e^{\alpha Y}} \exp\left(\frac{1}{\alpha_s^2 e^{\alpha Y}}\right) \Gamma\left(0, \frac{1}{\alpha_s^2 e^{\alpha Y}}\right) \\ &+ (\alpha_s^2 \alpha Y) \left\{ \frac{1}{\alpha_s^2 e^{\alpha Y}} \exp\left(\frac{1}{\alpha_s^2 e^{\alpha Y}}\right) \Gamma\left(0, \frac{1}{\alpha_s^2 e^{\alpha Y}}\right) \left[4 + \frac{10}{\alpha_s^2 e^{\alpha Y}} + \frac{3}{(\alpha_s^2 e^{\alpha Y})^2}\right] - \left[\frac{7}{\alpha_s^2 e^{\alpha Y}} + \frac{3}{(\alpha_s^2 e^{\alpha Y})^2}\right] \right\} \\ &+ (\alpha_s^2) \left\{ \tilde{f}_1(\alpha_s^2 e^{\alpha Y}) \right\} + (\alpha_s^2 \alpha Y)^2 \left\{ \tilde{f}_2(\alpha_s^2 e^{\alpha Y}) \right\} + \dots, \end{aligned} \quad (16)$$

however, it gets considerably simplified when  $\alpha_s^2 e^{\alpha Y}$  becomes large,

$$S(Y) = \frac{1}{\alpha_s^2 e^{\alpha Y}} \exp\left(\frac{1}{\alpha_s^2 e^{\alpha Y}}\right) \Gamma\left(0, \frac{1}{\alpha_s^2 e^{\alpha Y}}\right) \left[1 + 4\alpha_s^2 \alpha Y + \mathcal{O}\left(\frac{1}{\alpha_s^2 e^{\alpha Y}}\right)\right], \quad (17)$$

where  $\Gamma(0, x)$  is the incomplete gamma function. The NLO correction term  $4\alpha_s^2 \alpha Y$  inside the brackets with respect to the leading contribution is new.

## B. Method II: $\omega$ -representation

In this section, we develop another more powerful method, the  $\omega$ -representation, to solve the toy model. This method exhibits the pole-structure of the toy model which bears some resemblance to the pole-structure of the BFKL equation in QCD. The  $\omega$ -representation is equivalent to the integral representation method in

Sec. III A, however, it enables us to go one step further by resumming all the  $\alpha_s^2 \alpha Y$  terms in the  $S$ -matrix. Therefore, this method allows us to get an expression for the  $S$ -matrix which is assumed to be valid up to the rapidity  $Y_{c2} = \frac{1}{\alpha_s^4 \alpha}$  where the next-to-next-to-leading order ( $\mathcal{O}(\alpha_s^4) \alpha Y$ ) becomes of order one.

Let us show how to solve Eq. (2) with the  $\omega$ -representation method. One starts with the Laplace

transform of Eq. (2)

$$\omega n^{(k)}(\omega) - n^{(k)}(t) \Big|_{t=0} = kn^{(k)}(\omega) + k(k-1)n^{(k-1)}(\omega) - k\alpha_s^2 n^{(k+1)}(\omega), \quad (18)$$

where we have used the definitions  $t = \alpha y$  and  $n^{(k)}(\omega) = \int_0^\infty dt n^{(k)}(t) e^{-\omega t}$ . With the initial condition  $n_0^{(1)} \Big|_{y=0} = N$  and  $n_0^{(k)} \Big|_{y=0}^{k>1} = 0$ , Eq. (18) can be written into a matrix form:

$$\begin{pmatrix} \omega - 1 & \alpha_s^2 & 0 & 0 & 0 \\ -2 & \omega - 2 & 2\alpha_s^2 & 0 & 0 \\ 0 & \dots & \dots & \dots & 0 \\ 0 & 0 & -k(k-1) & \omega - k & k\alpha_s^2 \\ 0 & 0 & 0 & \dots & \dots \end{pmatrix} \cdot \begin{pmatrix} n^{(1)}(\omega) \\ n^{(2)}(\omega) \\ \dots \\ n^{(k)}(\omega) \\ \dots \end{pmatrix} = \begin{pmatrix} N \\ 0 \\ 0 \\ 0 \\ 0 \end{pmatrix}. \quad (19)$$

It is fairly complicated to solve this equation directly because of the infinite dimension it has. Nevertheless, there are two ways to attack this problem. First, we can follow the idea that the  $\alpha_s^2$  is small, which reduces the importance of recombination at the beginning of the evolution. Then we can solve the above linear algebra equation perturbatively which will prove that this approach is completely equivalent to the integral representation method we developed in the previous section. Second, noticing that Eq. (19) has an exact solution at finite dimensions, we can truncate the Eq. (19) to a  $k \times k$  linear algebra equation and then take the  $k \rightarrow \infty$  limit to get the solution of our infinite dimension matrix.

First, let us turn off the perturbation and only solve the unperturbed matrix to get the corresponding  $n_0^{(k)}(\omega)$ . One can easily find the solution to be  $n_0^{(k)}(\omega) = \frac{N(k-1)!k!}{(\omega-1)(\omega-2)\dots(\omega-k)} = \frac{N(k-1)!k!\Gamma(\omega-k)}{\Gamma(\omega)}$ . After the inverse Laplace transformation,

$$n_0^{(k)}(\alpha y) = \frac{1}{2\pi i} \int_{s-i\infty}^{s+i\infty} d\omega e^{\omega \alpha y} n_0^{(k)}(\omega), \quad (20)$$

$$= Nk! e^{k\alpha y} (1 - e^{-\alpha y})^{k-1}, \quad (21)$$

the result is exactly the same as what we have obtained in the previous section.

Turning on the perturbation, we find that the first-order correction  $\Delta n_1^{(k)}(\omega)$  to  $n_0^{(k)}(\omega)$  satisfies the equation:

$$\begin{pmatrix} \omega - 1 & 0 & 0 & 0 & 0 \\ -2 & \omega - 2 & 0 & 0 & 0 \\ 0 & \dots & \dots & 0 & 0 \\ 0 & 0 & -k(k-1) & \omega - k & 0 \\ 0 & 0 & 0 & \dots & \dots \end{pmatrix} \cdot \begin{pmatrix} \Delta n_1^{(1)}(\omega) \\ \Delta n_1^{(2)}(\omega) \\ \dots \\ \Delta n_1^{(k)}(\omega) \\ \dots \end{pmatrix} = \begin{pmatrix} -\alpha_s^2 n_0^{(2)}(\omega) \\ -2\alpha_s^2 n_0^{(3)}(\omega) \\ \dots \\ -k\alpha_s^2 n_0^{(k+1)}(\omega) \\ \dots \end{pmatrix}. \quad (22)$$

The general solution of this equation is too complicated to be written down. However, the strategy of how to get it is straightforward. For example, we can easily obtain  $\Delta n_1^{(1)}(\omega) = \frac{-2\alpha_s^2 N}{(\omega-1)^2(\omega-2)}$  which corresponds to the one-loop diagram. It yields the same result as given in Eq. (6) after the inverse Laplace transformation. This example shows that the result for each diagram calculated in the previous section becomes pretty much simplified in the  $\omega$ -representation. To see this more clearly, one can do the

Laplace transform of Eq. (11) and Eq. (12) which yields

$$\Delta n_m^{(k)}(\omega) = \frac{-k\alpha_s^2}{\omega - k} \Delta n^{(k+1)}(\omega), \quad (23)$$

$$\Delta n_s^{(k)}(\omega) = \frac{k(k-1)}{\omega - k} \Delta n^{(k-1)}(\omega). \quad (24)$$

According to these equations, one can directly write down the contribution for any diagram in this  $\omega$ -representation since the merging of  $k+1$ -particles to  $k$ -particles is nothing but adding a  $\frac{1}{\omega-k}$  pole with a prefactor  $-k\alpha_s^2$  in  $\omega$ -complex plane and the splitting of  $k-1$ -particles to  $k$ -particles is nothing but adding a  $\frac{1}{\omega-k}$  pole with a pref-

actor  $k(k-1)$ . Although the problem has been simplified a lot in the  $\omega$ -representation, the exact solution to

Eq. (19) is nevertheless unavailable this way.

---

We get the solution to Eq. (19) as follows: We first truncate the infinite dimension matrix (19) into a finite  $k \times k$  matrix, then exactly solve the amputated equation. Let us show the solutions for the first four  $k$ -values:

- $k = 1$  case: One obtains  $n_{1 \times 1}^{(1)}(\omega) = \frac{N}{\omega-1}$  which transforms to  $n_0^{(1)}(\alpha Y) = Ne^{\alpha Y}$ .
- $k = 2$  case: One obtains  $n_{2 \times 2}^{(1)}(\omega) = \frac{N(\omega-2)}{(\omega-1)(\omega-2)+2\alpha_s^2}$  which transforms to

$$n_1^{(1)}(\alpha Y) = \frac{1-2\alpha_s^2}{1-4\alpha_s^2} Ne^{(1+2\alpha_s^2)\alpha Y} - \frac{2\alpha_s^2}{1-4\alpha_s^2} Ne^{(2-2\alpha_s^2)\alpha Y}. \quad (25)$$

- $k = 3$  case: One obtains  $n_{3 \times 3}^{(1)}(\omega) = \frac{N[(\omega-2)(\omega-3)+12\alpha_s^2]}{(\omega-1)(\omega-2)(\omega-3)+2\alpha_s^2(7\omega-9)}$ . Then one can set the determinant  $(\omega-1)(\omega-2)(\omega-3)+2\alpha_s^2(7\omega-9) = 0$  which yields three solutions. Each of those three solutions stands for three poles  $\omega_1 = 1+2\alpha_s^2$ ,  $\omega_2 = 2+10\alpha_s^2$  and  $\omega_3 = 3-12\alpha_s^2$ , respectively. The inverse Laplace transform changes the integer exponents to non-integer renormalized exponents,

$$n_2^{(1)}(\alpha Y) = \frac{1+3\alpha_s^2}{1+\alpha_s^2} Ne^{(1+2\alpha_s^2)\alpha Y} - \frac{2\alpha_s^2+100\alpha_s^4}{1-14\alpha_s^2} Ne^{(2+10\alpha_s^2)\alpha Y} + \frac{72\alpha_s^4}{1-31\alpha_s^2} Ne^{(3-12\alpha_s^2)\alpha Y}. \quad (26)$$

- $k = 4$  case: One obtains  $n_{4 \times 4}^{(1)}(\omega) = \frac{N[(\omega-2)(\omega-3)(\omega-4)+24\alpha_s^2(2\omega-5)]}{(\omega-1)(\omega-2)(\omega-3)(\omega-4)+2\alpha_s^2(72-91\omega+25\omega^2)+72\alpha_s^4}$ . The denominator has 4 poles which are  $\omega_1 = 1+2\alpha_s^2 + o(\alpha_s^4)$ ,  $\omega_2 = 2+10\alpha_s^2 + o(\alpha_s^4)$ ,  $\omega_3 = 3+24\alpha_s^2+1164\alpha_s^4$  and  $\omega_4 = 4-36\alpha_s^2-1080\alpha_s^4$ . Then, the inverse Laplace transform gives

$$n_3^{(1)}(\alpha Y) = N(1+o(\alpha_s^2))e^{(1+2\alpha_s^2)\alpha Y} - 2!N\alpha_s^2(1+o(\alpha_s^2))e^{(2+10\alpha_s^2)\alpha Y} + 3!N\alpha_s^4(1+o(\alpha_s^2))Ne^{(3+24\alpha_s^2)\alpha Y} - 7344(\alpha_s^6)Ne^{(4-36\alpha_s^2)\alpha Y}. \quad (27)$$

---

From the above calculation for  $n^{(1)}(\alpha Y)$ , one can already see that for an arbitrary  $k$ , the first  $k-1$  poles are stabilized to the corresponding solutions  $\omega_j = j+(3j^2-j)\alpha_s^2 + \mathcal{O}(\alpha_s^4)$  ( $1 \leq j \leq k$ ) with a fixed coefficient  $j!N(\alpha_s^2)^{j-1}$  and the last pole is always  $\omega_k = k-k(k-1)^2\alpha_s^2 + \mathcal{O}(\alpha_s^4)$  with a wrong coefficient since it misses the recombination from  $(k+1)$  particle mode as a result of truncation at the  $k$  particle mode. In addition, it is easy to see that the  $(3j^2-j)\alpha_s^2$  term is corresponding to the sum of the

---

NLO contributions  $(j+1)j^2\alpha_s^2\alpha Y$  of the leading loop diagrams (e.g. Fig. 1 B) and the leading contributions  $(-j(j-1)^2)\alpha_s^2\alpha Y$  of the NLO loop diagrams (Fig. 1 C). On the other hand, the  $-k(k-1)^2\alpha_s^2$  term in the last pole only corresponds to the leading order contributions of the NLO loop diagrams (e.g. Fig. 1 C) as a consequence of the truncation at dimension  $k$  which rules out the leading loop diagram but allows the NLO loop diagrams at the  $k$  particle mode.

---

The pattern of the exact solution is transparent from the above discussion and the generalization to infinite dimensions follows by simply taking the limit  $k \rightarrow \infty$ . The exact solution for the  $S$ -matrix in infinite dimensions reads

$$S_{exact}(\alpha Y) = \sum_{k=0}^{\infty} (-1)^k (\alpha_s^2)^k k! e^{(k+k(3k-1)\alpha_s^2)\alpha Y + \mathcal{O}(\alpha_s^4)\alpha Y} (1 + \mathcal{O}(\alpha_s^2)). \quad (28)$$

This result agrees with what we have found in the previous section, see Eq. (15), however, it goes a step further since the  $k(3k-1)\alpha_s^2\alpha Y$  term is now in the exponent which can be understood as a resummation of all  $\alpha_s^2\alpha Y$  terms via exponentiation in Eq. (15).

---

We notice that the  $S$ -matrix is not Borel-summable since  $e^{3\alpha_s^2\alpha Y k^2}$  is beyond the Borel-summability accord-

ing to Nevanlinna's theorem [23]. However, one can generalize the Borel-summation technique and show that the above series still has a finite sum by using analytic continuation. Generally speaking, one can see that the  $S$ -matrix is the analytic function of two independent variables,  $\alpha_s^2$  and  $\alpha Y$ , when  $\alpha_s^2$  is negative in the  $\alpha_s^2$  complex

plane. Since  $\alpha_s^2 = 0$  is not a singularity, one can use analytic continuation to define the other half plane when  $\alpha_s^2$  becomes positive. In the following, we provide a generalized Borel-summation method which yields a finite result.

We use a technique together with a subsequent Borel-summation in order to maneuver the divergent series Eq. (28) into a definite and well-defined sum. Let us define  $u = \alpha_s^2 e^{(1-\alpha_s^2)\alpha Y}$  and  $\gamma = 3\alpha_s^2\alpha Y$ , then we obtain

$$S(\alpha Y) = \sum_{k=0}^{\infty} (-1)^k k! u^k e^{\gamma k^2}, \quad (29)$$

$$= \sum_{k=0}^{\infty} (-1)^k \left( \frac{1}{u} \int_0^{\infty} db b^k e^{-\frac{b}{u}} \right) \left( \sqrt{\frac{\gamma}{\pi}} \int_{-\infty}^{+\infty} dx \exp(-\gamma x^2 + 2\gamma x k) \right), \quad (30)$$

$$= \sqrt{\frac{\gamma}{\pi}} \int_{-\infty}^{+\infty} dx \exp(-\gamma x^2) \frac{1}{u} \int_0^{\infty} db \exp\left(-\frac{b}{u}\right) \frac{1}{1 + b e^{+2\gamma x}}, \quad (31)$$

$$= \sqrt{\frac{\gamma}{\pi}} \int_{-\infty}^{+\infty} dx \exp(-\gamma x^2) \frac{1}{u e^{+2\gamma x}} \exp\left(\frac{1}{u e^{+2\gamma x}}\right) \Gamma\left(0, \frac{1}{u e^{+2\gamma x}}\right). \quad (32)$$

To check the convergence of this integral, one can expand  $\Gamma(0, z)$  at  $z \rightarrow \infty$  which gives  $\Gamma(0, z) \simeq \frac{\exp(-z)}{z} \left(1 - \frac{1}{z}\right)$ , showing that the above integral is definitely finite and well-defined. The  $x$ -integration can not be performed analytically. However, one can use the saddle point approximation to evaluate the above  $x$ -integral, in which one finds the saddle point  $x = -1$ , and

$$S(\alpha Y) = \sqrt{\frac{\gamma}{\pi}} \int_{-\infty}^{+\infty} dx \exp(-\gamma x^2 - 2\gamma x) \frac{1}{u} \exp\left(\frac{1}{u e^{+2\gamma x}}\right) \Gamma\left(0, \frac{1}{u e^{+2\gamma x}}\right) \quad (33)$$

$$\approx \frac{1}{\alpha_s^2 e^{(1-4\alpha_s^2)\alpha Y}} \exp\left(\frac{1}{\alpha_s^2 e^{(1-7\alpha_s^2)\alpha Y}}\right) \Gamma\left(0, \frac{1}{\alpha_s^2 e^{(1-7\alpha_s^2)\alpha Y}}\right). \quad (34)$$

A good agreement of this result with the numerical evaluation of Eq. (31) is shown in Fig. (2,3).

Eq. (34) is a fairly exact result in the high-energy limit since it presumably resums all the sub-leading diagrams up to  $\alpha_s^2\alpha Y$  level, only neglects  $\mathcal{O}(\alpha_s^2)$  (in the prefactor) and  $\mathcal{O}(\alpha_s^4\alpha Y)$  (in the exponent) corrections. If we compare this with Eq. (17) of the previous section, we can see that Eq. (17) is an approximate solution which results from Eq. (34) when  $\alpha_s^2\alpha Y \ll 1$ . The  $\omega$ -representation is equivalent to the integral representation method in Sec. III A, however, it enables us to go one step further by resumming all the  $\alpha_s^2\alpha Y$  terms in the  $S$ -matrix. Thus, the  $S$ -matrix in Eq. (34) is assumed to be valid up to the rapidity  $Y_{c2} = \frac{1}{\alpha_s^4\alpha}$  where the next-to-next-to-leading order ( $\mathcal{O}(\alpha_s^4\alpha Y)$ ) becomes of order one.

### C. The Consequences of the NLO Correction

In Mueller's toy model [1], which was inspired by the QCD dipole model (DM) [19], the  $S$ -matrix for particle-particle scattering in the center-of-mass frame is given

by

$$S^{DM}(Y) = \sum_{m,n=1}^{\infty} e^{-\alpha_s^2 mn} P_m\left(\frac{Y}{2}\right) P_n\left(\frac{Y}{2}\right), \quad (35)$$

where  $P_n(Y)$  is the probability density for having  $n$  particles in the wavefunction of an initial single particle after the evolution up to  $Y$ . For large rapidities,  $P_n(Y)$  reads [1]

$$P(n, Y) = \frac{1}{\bar{n}(Y)} e^{-n/\bar{n}(Y)} \quad (36)$$

with  $\bar{n}(Y) = \exp(\alpha_s Y)$ . Using  $u = n/\bar{n}(Y/2)$  and  $v = m/\bar{n}(Y/2)$  and changing the summations in eq. (35) into integrals (this change is rigorous since  $du=dv=1/\bar{n}(Y/2)$  is infinitesimal) for large rapidities, one obtains

$$S^{DM}(Y) = \int_{\frac{1}{\bar{n}(Y/2)}}^{\infty} du \int_{\frac{1}{\bar{n}(Y/2)}}^{\infty} dv \exp[-\alpha_s^2 \bar{n}(Y) uv - u - v] \quad (37)$$

which after the integration over  $u$  and  $v$  leads to

$$S^{DM}(Y) \simeq \frac{1}{\alpha_s^2 e^{\alpha Y}} \ln \left[ \frac{\alpha_s^2 e^{\alpha Y}}{(1 + \alpha_s^2 e^{\alpha Y/2})^2} \right]. \quad (38)$$

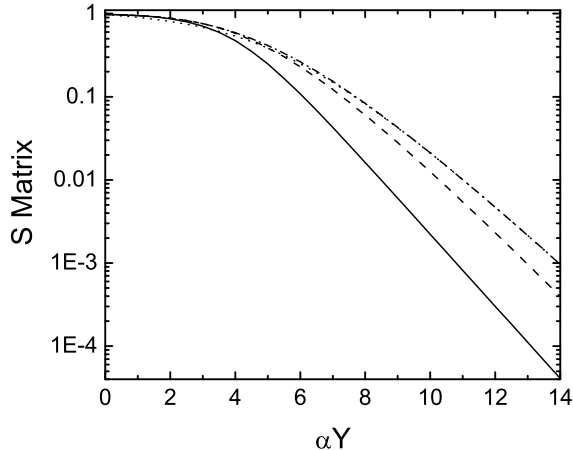


FIG. 2: The  $S$ -matrix as a function of  $\alpha Y$  for  $\alpha_s^2 = 0.02$  in logarithmic scale: The solid line represents the solution of the zero-transverse dimensional Kovchegov equation. The dashed line corresponds to the leading order result, the dotted line stands for the saddle point approximation (34) and the dot-dashed line is extracted from the numerical evaluation of Eq. (31).

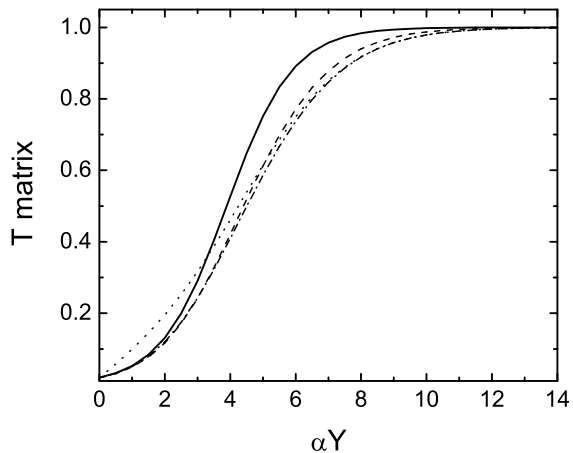


FIG. 3: The  $T$ -matrix as a function of  $\alpha Y$  for  $\alpha_s^2 = 0.02$ : The solid line represents the solution of the zero-transverse dimensional Kovchegov equation. The dashed line corresponds to the leading order result, the dotted line stands for the saddle point approximation (34) and the dot-dashed line is extracted from the numerical evaluation of Eq. (31).

This result reduces for  $Y \ll Y_s = \frac{2}{\alpha_s} \ln\left(\frac{1}{\alpha_s^2}\right)$  to

$$S^{DM}(Y) \simeq \frac{1}{\alpha_s^2 e^{\alpha Y}} \ln[\alpha_s^2 e^{\alpha Y}] \quad (39)$$

while for  $Y \gg Y_s$  it gets

$$S^{DM}(Y) \simeq \frac{1}{\alpha_s^2 e^{\alpha Y}} \ln\left[\frac{1}{\alpha_s^2}\right]. \quad (40)$$

It is easy to see that the result in Eq. (38) agrees with our LO contribution given in Eq. (17) only when  $Y \leq Y_s$ . For  $Y \gg Y_s$  the result from Mueller's toy model given in Eq. (40) can not be trusted since it does not include saturation effects within the interacting particle wave functions which start becoming important at  $Y \simeq Y_s$ . Mueller's toy model fails to reproduce the LO contribution of the LO diagrams (e.g. Fig 1 B) at  $Y \gg Y_s$ , it does not include the NLO contribution of the LO diagrams (terms including  $(k-1)^2 \alpha Y / e^{\alpha Y}$  in Eq. (13)) and it also misses the NLO loop diagrams (e.g. Fig 1 C).

Mueller and Salam [2] have been able to calculate the probability distribution  $P_n(Y)$  which includes saturation effects by imposing boost invariance on the small- $x$  evolution. They calculated the boost invariant  $S$  matrix in the rest frame of the target, and obtained the same LO result in Eq. (17). We also find that it is interesting to calculate the  $S$  matrix in the center of mass frame. Inserting their result,

$$P^s(n, y) = \exp\left[\alpha_s^2 n - \alpha y - \frac{1}{\alpha_s^2} \left(e^{\alpha_s^2 n} - 1\right) e^{-\alpha y}\right] \quad (41)$$

in Eq. (35), converting the summations into integrals, changing the integration variables from  $m-1$  to  $m$  and from  $n-1$  to  $n$ , setting  $e^{\alpha_s^2} = 1$ , and using the integration variables  $v = n/\bar{n}(Y/2)$  and  $u = m/\bar{n}(Y/2)$ , one ends up with the boost-invariant result for the  $S$ -matrix in the center of mass frame,

$$S^B(Y) \simeq \int_0^\infty du \int_0^\infty dv \exp[-\alpha_s^2 \bar{n}(Y) uv - u - v] \quad (42)$$

$$= \frac{1}{\alpha_s^2 e^{\alpha Y}} e^{\frac{1}{\alpha_s^2 e^{\alpha Y}}} \Gamma\left(0, \frac{1}{\alpha_s^2 e^{\alpha Y}}\right) \quad (43)$$

$$\simeq \frac{1}{\alpha_s^2 e^{\alpha Y}} \ln[\alpha_s^2 e^{\alpha Y}]. \quad (44)$$

This result agrees with our LO contribution in Eq. (17). Note, however, that the Mueller-Salam toy model does not incorporate the NLO correction given in Eq. (17). Our toy model, Eq. (17), tells us that the NLO correction is negligible for  $Y \leq Y_c = \frac{1}{\alpha \alpha_s^2}$ . This means that the result in Eq. (43) is valid over a much larger rapidity range, up to  $Y \simeq Y_c = \frac{1}{\alpha \alpha_s^2}$ , as compared to the result in (38) which is inspired from the dipole model and which breaks down at  $Y_s = \frac{2}{\alpha_s} \ln\left(\frac{1}{\alpha_s^2}\right)$ . Therefore, the effect of saturation is to replace the result in Eq. (40) by the



result in Eq. (39) even when  $Y \geq Y_s$ . It is interesting to note that the saturation effects are mathematically included by setting the lower limits in Eq. (37) to 0 as can be seen by comparing Eq. (37) with Eq. (42) without modifying the probability distribution. (In addition, one can easily prove that the  $S$  matrix of dipole approach is boost invariant if and only if the lower limits in Eq. (37) are set to 0.)

#### IV. CONCLUSION

We have investigated a stochastic toy model without transverse dimensions (equivalently, a infinite dimension hierarchy of evolution equation) which naturally generates Pomeron loops. We have computed the Pomeron loop diagrams to the NLO using two different methods. We find that the LO calculation agrees with the existing results in the literature [1, 2]. The study of NLO graphs in this toy model generates the  $(\alpha_s^2 \alpha Y)$  corrections.

Observations made by investigating Mueller's toy model [1] have been shown numerically by Salam [20, 21] to be valid also in the four-dimensional QCD. Presumably our toy model reveals properties of the four-dimensional QCD evolution to some extent. We believe that the NLO correction in the four-dimensional QCD would be of order  $\alpha_s^2 \alpha Y$  as well (here we define  $\alpha = \alpha_P - 1 = \frac{4\alpha_s N_c}{\pi} \ln 2$  to be the BFKL pomeron intercept). The behavior of our toy model is heuristically indicating that NLO contributions can be neglected in the four-dimensional QCD evolution as long as  $Y \ll Y_c$  as well. This believe is strengthened even more by noticing that the NLO correction  $\alpha_s^2 \alpha Y$  seem to naturally appear in QCD: There are two types of NLO contributions.

- The first type of NLO contribution comes from NLO contribution of LO graphs (see example Fig. 1 B). For the one-loop diagram, for instance, the LO contribution in QCD is  $(\alpha_s^2)^2 \exp(2\alpha Y)$  which comes from varying the size of the loop from 0 to  $Y$ . The NLO contribution  $(\alpha_s^2)^2 \alpha Y \exp(\alpha Y)$  comes from changing the location of a fixed zero-size loop from 0 to  $Y$ . The NLO contribution is suppressed by the factor  $\alpha Y / e^{\alpha Y}$  with respect to the LO contribution, as in the toy model (see Eq. (13)), leading to the general form  $\alpha_s^2 \alpha Y$ .
- The second type of NLO contribution comes from LO contribution of NLO graphs (see example Fig. 1 C). For the two-loop diagram Fig. 1 C, for instance, the LO contribution  $(\alpha_s^2)^3 \alpha Y \exp(2\alpha Y)$  comes from shifting the location of the fixed zero-size connecting Pomeron between two loops from 0 to  $Y$  while the sizes of these two loops are changed in the same time. Since the total amplitude of this graph does not depend on the location of the connecting Pomeron, one can obtain an extra factor

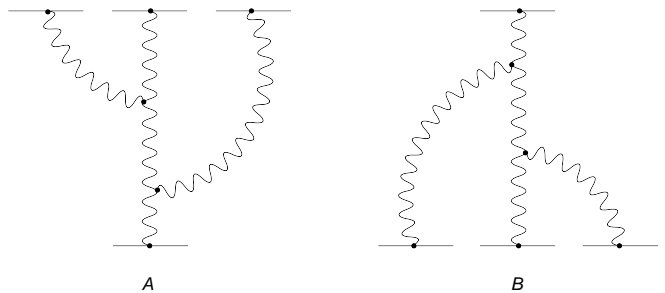


FIG. 4: Graphs for one object scattering with three objects. Curly lines represent BFKL ladders. In graph (A) a single particle evolves through Pomeron splittings and scatters off three particles, while in graph (B) three particles evolve through Pomeron mergings and scatter off a single particle.

of  $\alpha Y$  by integrating from 0 to  $Y$ . The NLO contribution (see Eq. (14)) is suppressed by the factor  $\alpha Y / e^{\alpha Y}$  with respect to the LO contribution of Fig. 1 B, as in the toy model (see Eq. (13)), leading to the general form  $\alpha_s^2 \alpha Y$ .

Therefore, we can see that the NLO correction generally takes the form of  $\alpha_s^2 \alpha Y$ . A QCD model in which all Pomeron splittings occur before all Pomeron mergings in a boost-invariant manner (as in this toy model) would lead to the right LO result which would be valid up to the limit  $\frac{1}{\alpha \alpha_s^2}$ .

#### Acknowledgments

We would like to thank Alfred Mueller for numerous stimulating and insightful discussions. We are also grateful to Stephane Munier for many useful remarks and comments. A. Sh. acknowledges financial support by the Deutsche Forschungsgemeinschaft under contract Sh 92/2-1.

#### APPENDIX A: THE EQUIVALENCE OF SPLITTING AND RECOMBINATION

In this part, we show that Eq. (2) gives Lorentz invariant results. To show this, let us start with a single particle, then split it to three particles which yields  $n_0^{(3)}(y) = N3!e^{3\alpha y}(1 - e^{-\alpha y})^2$  according to Eq. (4). Following Kovchegov [24], the scattering amplitude is

$$A(\alpha Y) = \sum_{k=1}^{\infty} \frac{(-1)^{k+1}}{k!} n_0^{(k)}(Y) T^{(k)}(0). \quad (\text{A1})$$

in which  $T^{(k)}(0) = (\alpha_s^2)^k$  and the  $\frac{1}{k!}$  can be understood as the fact that those  $k$ -particles in the target are the same. Therefore, it is very easy to see that  $A_s(\alpha Y) =$

$N (\alpha_s^2 e^{\alpha y})^3 (1 - e^{-\alpha y})^2$  which corresponds to the diagram shown in Fig. 4 A.

On the other hand, we can put the evolution into the target, let them merge into one object before scattering with the projectile (Fig. 4 B). This means that one starts with an initial condition  $n_0^{(3)}|_{y=0} = N_3$  and  $n_0^{(k)}|_{y=0}^{k \neq 3} = 0$  in solving the Eq. (2). After merging twice from  $n_0^{(3)}(y) = N_3 e^{3\alpha y}$ , one obtains  $\Delta n^{(1)} = N_3 \left(\frac{\beta}{\alpha}\right)^2 e^{3\alpha y} (1 - e^{-\alpha y})^2$ . Finally, it is straight forward

to see that  $A_m(\alpha Y) = N_3 (\alpha_s^2 e^{\alpha y})^3 (1 - e^{-\alpha y})^2$  after setting  $\frac{\beta}{\alpha} = \alpha_s^2$ . Presumably,  $A_s(\alpha Y)$  should be same as  $A_m(\alpha Y)$  since they actually describe the same process, and they are indeed the same once we set  $N = N_3$ .

Moreover, it is tempting to replace the target by a large nucleus with  $A$  nucleons inside it. Then, we need to define  $T^{(k)}(0) = \left(A^{\frac{1}{3}} \alpha_s^2\right)^k$ , and indeed one can see that  $A_s(\alpha Y) = A_m(\alpha Y)$  as long as we set  $N_3 = N \left(A^{\frac{1}{3}}\right)^3$ .

---

## APPENDIX B: SOLUTION TO A SLIGHTLY DIFFERENT STOCHASTIC DIFFERENTIAL EQUATION

We notice that there has been a lot of theoretical discussion and numerical simulation on a slightly different stochastic differential equation which has a noise term  $\sqrt{2(\alpha\tilde{n} - \beta\tilde{n}^2)}\nu(y)$ , namely the stochastic Fisher-Kolmogorov-Petrovsky-Piscounov (sFKPP) equation. For completeness, we provide the solution to this equation by using the  $\omega$ -representation we developed above. The dynamics of this equation is given by two random processes: by an increase  $dY$  in rapidity, a particle can split into two particles with some rate  $\alpha$  ( $A \xrightarrow{\alpha} A + A$ ) or two particles can merge into one with a rate  $2\beta$  ( $A + A \xrightarrow{2\beta} A$ ). From the equation,

$$\frac{d\tilde{n}}{dy} = \alpha\tilde{n} - \beta\tilde{n}^2 + \sqrt{2(\alpha\tilde{n} - \beta\tilde{n}^2)}\nu(y), \quad (\text{B1})$$

one can get

$$\frac{dn^{(k)}}{dy} = (k\alpha - k(k-1)\beta)n^{(k)} + k(k-1)\alpha n^{(k-1)} - k\beta n^{(k+1)}. \quad (\text{B2})$$

Similarly, one can write Eq. (B2) into a matrix in the  $\omega$ -representation, then get the similar  $S$ -matrix of the scattering between two dipoles,

$$S(\alpha Y) = \sum_{k=0}^{\infty} (-1)^k (\alpha_s^2)^k k! e^{(k+2k^2\alpha_s^2)\alpha Y + o(\alpha_s^4)\alpha Y} (1 + o(\alpha_s^2)), \quad (\text{B3})$$

$$= \sqrt{\frac{\delta}{\pi}} \int_{-\infty}^{+\infty} dx \exp(-\delta x^2) \frac{1}{ve+2\delta x} \exp\left(\frac{1}{ve+2\delta x}\right) \Gamma\left(0, \frac{1}{ve+2\delta x}\right) \quad (\text{B4})$$

$$\approx \frac{1}{\alpha_s^2 e^{(1-2\alpha_s^2)\alpha Y}} \exp\left(\frac{1}{\alpha_s^2 e^{(1-4\alpha_s^2)\alpha Y}}\right) \Gamma\left(0, \frac{1}{\alpha_s^2 e^{(1-4\alpha_s^2)\alpha Y}}\right), \quad (\text{B5})$$

where  $\delta = 2\alpha_s^2\alpha Y$  and  $v = \alpha_s^2 e^{\alpha Y}$ . The difference of between this result and the one in Eq. (34) is at the NLO correction, however, one can see that Eq. (1) has a more transparent physical meaning in QCD since it contains the projectile-target duality and one can easily relate it to the zero transverse dimension reggeon theory.

---

- [1] A. H. Mueller, Nucl. Phys. B **437** (1995) 107.  
[2] A. H. Mueller and G. P. Salam, Nucl. Phys. B **475**, 293 (1996).  
[3] A. H. Mueller and A. I. Shoshi, Nucl. Phys. B **692** (2004) 175.  
[4] E. Iancu, A. H. Mueller and S. Munier, Phys. Lett. B **606** (2005) 342.

- [5] S. Munier and R. Peschanski, Phys. Rev. Lett. **91** (2003) 232001; Phys. Rev. D **69** (2004) 034008.  
[6] E. Iancu and D. N. Triantafyllopoulos, Nucl. Phys. A **756** (2005) 419.  
[7] I. Balitsky, Nucl. Phys. B **463** (1996) 99; Phys. Rev. Lett. **81** (1998) 2024; Phys. Lett. B **518** (2001) 235.  
[8] J. Jalilian-Marian, A. Kovner, A. Leonidov and

- H. Weigert, Nucl. Phys. B **504** (1997) 415; Phys. Rev. D **59** (1999) 014014.
- E. Iancu, A. Leonidov and L. D. McLerran, Phys. Lett. B **510** (2001) 133; Nucl. Phys. A **692** (2001) 583.
- H. Weigert, Nucl. Phys. A **703** (2002) 823.
- [9] A. H. Mueller, A. I. Shoshi and S. M. H. Wong, Nucl. Phys. B **715** (2005) 440.
- [10] E. Iancu and D. N. Triantafyllopoulos, Phys. Lett. B **610** (2005) 253.
- [11] A. Kovner and M. Lublinsky, Phys. Rev. D **71** (2005) 085004.
- [12] Y. Hatta, E. Iancu, L. McLerran, A. Stasto and D. N. Triantafyllopoulos, arXiv:hep-ph/0504182.
- [13] A. Kovner and M. Lublinsky, Phys. Rev. Lett. **94** (2005) 181603; JHEP **0503** (2005) 001; Phys. Rev. D **72** (2005) 074023; “More remarks on high energy evolution,” arXiv:hep-ph/0510047.
- [14] J. P. Blaizot, E. Iancu, K. Itakura and D. N. Triantafyllopoulos, Phys. Lett. B **615** (2005) 221.
- Y. Hatta, E. Iancu, L. McLerran and A. Stasto, Nucl. Phys. A **762** (2005) 272.
- E. Iancu, G. Soyez and D. N. Triantafyllopoulos, “On the probabilistic interpretation of the evolution equations with Pomeron arXiv:hep-ph/0510094.
- [15] C. Marquet, A. H. Mueller, A. I. Shoshi and S. M. H. Wong, Nucl. Phys. A **762** (2005) 252.
- [16] E. Levin and M. Lublinsky, “Towards a symmetric approach to high energy evolution: Generating functional with Pomeron loops,” arXiv:hep-ph/0501173. E. Levin, Nucl. Phys. A **763**, 140 (2005).
- [17] R. Enberg, K. Golec-Biernat and S. Munier, Phys. Rev. D **72** (2005) 074021.
- [18] G. Soyez, Phys. Rev. D **72** (2005) 016007.
- [19] A. H. Mueller, Nucl. Phys. B **415** (1994) 373; Nucl. Phys. B **425** (1994) 471.
- [20] G. P. Salam, Nucl. Phys. B **461** (1996) 512;
- [21] G. P. Salam, Nucl. Phys. B **449** (1995) 589.
- [22] Y. V. Kovchegov, Phys. Rev. D **72** (2005) 094009.
- [23] G.H. Hardy, Divergent Series(Oxford University, Oxford, 1963).
- [24] Y. V. Kovchegov, Phys. Rev. D **60** (1999) 034008.